J. Membrane Biol. 83, 95–107 (1985)

The Journal of
Membrane Biology


# Complex Subcellular Distributions of Enzymatic Markers in Intestinal Epithelial Cells

Austin K. Mircheff,† Dennis J. Ahnen,‡·* Anisul Islam,† Nilda A. Santiago,‡ and Gary M. Gray‡
†Department of Physiology and Biophysics, University of Southern California School of Medicine, Los Angeles, California 90033
and ‡Division of Gastroenterology, Department of Medicine, Stanford University School of Medicine, Stanford, California 94305

**Summary.** Current procedures for isolating intestinal epithelial cell surface and intracellular membranes are based on the assumption that each organelle is marked by some unique constituent. This assumption seemed inconsistent with the dynamic picture of subcellular organization emerging from studies of membrane turnover and recycling. Therefore, we have designed an alternative fractionation which is independent of *a priori* marker assignments. We subjected mucosal homogenates to a sequence of separations based on sedimentation coefficient, equilibrium density, and partitioning in aqueous polymer two-phase systems. The resulting distributions of protein and enzymatic markers define a total of 17 physically and biochemically distinct membrane populations. Among these are: basal-lateral membranes, with Na,K-ATPase enriched 21-fold; brush-border membranes, with alkaline phosphatase enriched as much as 38-fold; two populations apparently derived from the endoplasmic reticulum; a series of five populations believed to have been derived from the Golgi complex; and a series of five acid phosphatase-rich populations which we cannot identify unequivocally. Each of the five enzymatic markers we have followed is associated with a multiplicity of membrane populations. Basal-lateral, endoplasmic reticulum, and Golgi membranes contain alkaline phosphatase at the same specific activity as the initial homogenate. Similarly, Na,K-ATPase appears to be associated with Golgi, endoplasmic reticulum, and brush-border membranes at specific activities two- to seven-fold that of the initial homogenate.

**Key Words:** brush border · basal-lateral membranes · endoplasmic reticulum · Golgi · phase partitioning

## Introduction

The ability of the intestinal epithelium to perform its surface hydrolytic and absorptive functions depends on the asymmetric distributions of membrane constituents between the apical- and basal-lateral plasma membranes. Hydrolases and sodium-coupled transport systems for a variety of substrates are concentrated in the apical plasma membranes, while Na,K-ATPase and equilibrating systems for sugars and amino acids are concentrated in the basal-lateral membranes [e.g., 15, 28]. It is becoming evident that a good deal of structural complexity underlies this simple functional principle. We know that there is an ongoing flux of membrane glycoproteins from their intracellular sites of synthesis and assembly to the brush-border membranes [1, 2, 5], and, presumably, to intracellular loci where they are degraded. Ultrastructural studies in a variety of cell types have also demonstrated that receptors may recycle between the plasma membranes and intracellular compartments [e.g., 10, 25]. The existence of such phenomena emphasizes the importance of the mechanisms that establish and maintain epithelial polarity; at the same time, it suggests possible mechanisms for regulation of intestinal function. That is, the plasma membrane's content of a transport protein or surface hydrolytic enzyme could be increased by increased rates of synthesis, decreased rates of degradation, or redistribution from preformed, intracellular pools.

Samples of isolated plasma membranes are widely used for studies of intestinal absorptive mechanisms. It would be essential to have samples of all the participating subcellular membranes in order to begin evaluating the physical and biochemical mechanisms of the membrane biogenetic phenomena. Despite the complexity of intracellular biochemical organization implied by the turnover and recycling of plasma membrane constituents, current procedures for isolating intestinal subcellular membranes are based on the assumption that each organelle is marked by a unique biochemical constituent. As an alternative to this conceptual approach, we have followed an empirical strategy [16] based on the premise that when cells are disrupted, the populations of membranes derived from different organ-

* *Present address:* Section of Gastroenterology, Department of Medicine, Veterans Administration Medical Center, Denver, Colorado 94121.

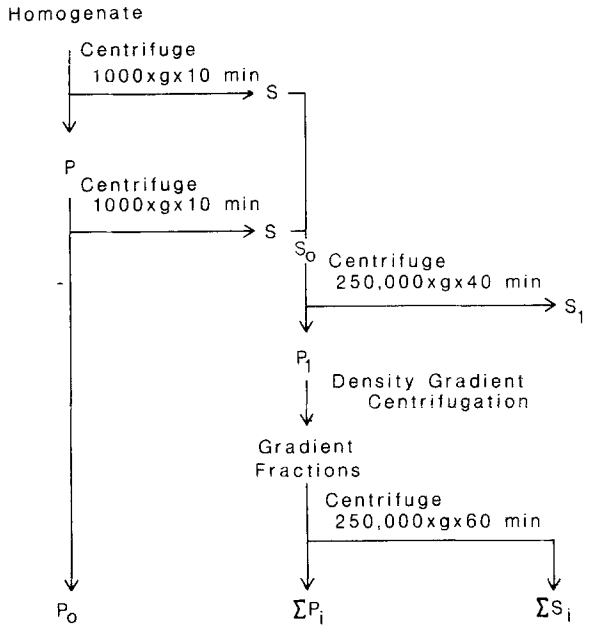


**Fig. 1.** Summary of differential and density gradient centrifugation procedures. Membranes harvested from the density gradient fractions ($\Sigma P_i$) were subsequently pooled and subjected to counter-current distribution

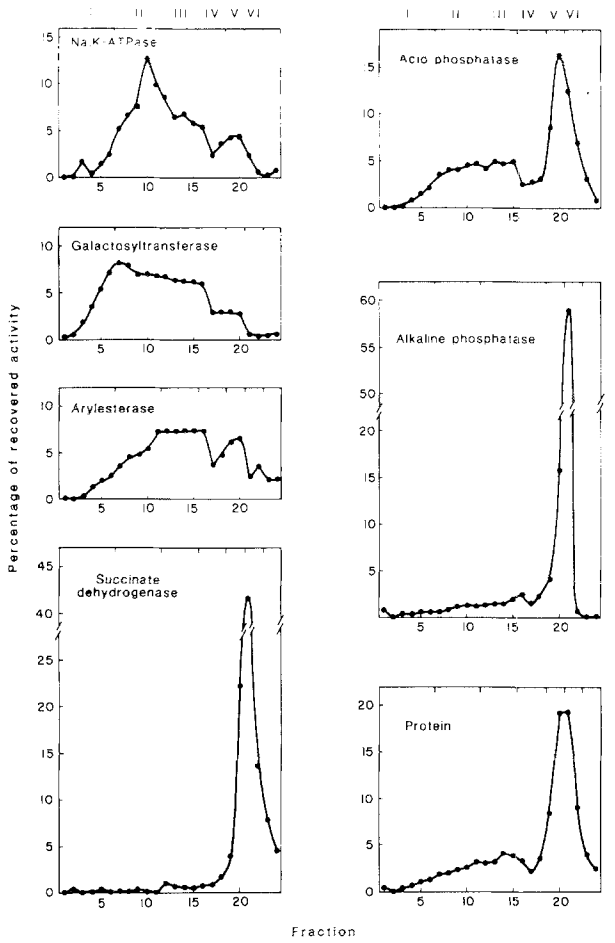


**Fig. 2.** Density distributions of protein and enzymatic markers. Density gradient centrifugation was performed in a Z-60 zonal rotor as described under Materials and Methods; the sample layer corresponds to fractions 10 to 15

elles are characterized by unique sets of physical properties and unique combinations of constituents, each of which might be shared with other membrane populations. This strategy represents a return to the fundamental principles expressed in DeDuve's theoretical work [7]. Its essence is that when separation procedures are used as analytical tools, it is possible to distinguish and characterize membrane populations without invoking the postulate of unique marker localizations. We have now combined separation procedures based on a total of four different physical properties to delineate the major populations of membranes present in intestinal mucosal homogenates. These include brush-border and basal-lateral plasma membranes, several populations that appear to be derived from Golgi and endoplasmic reticulum membranes, and a complex of membrane populations whose subcellular origins we cannot yet identify. The result represents both a new method for isolating intestinal subcellular components and a new picture of the intestinal epithelial cell's internal biochemical organization.

## Materials and Methods

One 240 to 260 g male Sprague-Dawley rat was used in each experiment. It was fasted overnight, then killed by cervical dislocation. The entire small intestine was perfused with ice-cold 150 mM NaCl. The duodenum and ileum, i.e., the proximal and distal 15 cm, were discarded, and the remaining jejunum was cut longitudinally. It was placed in ice-cold 150 mM NaCl and shaken at moderate speed, with six changes of solution, for 30 min to remove adhering mucus. The perfusion and wash solutions contained 1 mM dithiothreitol, as suggested by Weiser [31], to promote dissociation of mucus. The last wash solution also included 0.2 mM phenylmethylsulfonyl fluoride to inhibit residual pancreatic protease activity. The mucosa was removed by scraping with a glass slide, resuspended in 60 ml Isolation Buffer (5% sorbitol, 0.5 mM NaEDTA and 5 mM histidine-imidazole, pH 7.5), and centrifuged at 500 × $g$ × 5 min.

The homogenization, differential sedimentation, and density gradient centrifugation procedures were similar to those devised for an analytical fractionation of the rat exorbital lacrimal gland [17, 19]. The mucosal scrapings were resuspended in 150 ml isolation buffer and homogenized with a Tissumiser (Tekmar Co.) run at low speed for 10 min. Differential sedimentation, outlined in Fig. 1, was used to separate the homogenate into three Sedimentation Windows: $P_o$, which contained material sedimenting at 1000 × $g$ × 10 min; $\Sigma P_i$, which contained material sedimenting between 1000 × $g$ × 10 min and 250,000 × $g$ × 40 min; and $S_1 + \Sigma S_i$, which contained material failing to sediment

**Table 1.** Distribution of biochemical markers during differential sedimentation[a]

| | $P_o$ | $S_1$ | $\Sigma S_i$ | $\Sigma P_i$ | Recovery from $S_o$ | Recovery from $P_1$ |
|---|---|---|---|---|---|---|
| Na,K-ATPase | 2.8 ± 4.8 | 1.5 ± 1.6 | 5.1 ± 4.5 | 90.1 ± 9.5 | 71.6 ± 29.9 | 90.7 ± 16.5 |
| Alkaline phosphatase | 31.9 ± 16.2 | 1.5 ± 1.1 | 12.8 ± 7.1 | 53.9 ± 9.5 | 85.0 ± 20.4 | 85.3 ± 26.1 |
| Acid phosphatase | 11.9 ± 6.9 | 16.1 ± 9.8 | 15.0 ± 10.8 | 57.8 ± 11.1 | 79.9 ± 17.0 | 77.6 ± 15.4 |
| Galactosyltransferase | 8.5 ± 2.8 | 5.9 ± 0.8 | 35.5 ± 13.6 | 64.5 ± 3.1 | 102.2 ± 50.2 | 93.4 ± 24.5 |
| Protein | 14.1 ± 3.8 | 47.4 ± 4.7 | 17.1 ± 3.5 | 21.1 ± 2.0 | 91.7 ± 6.5 | 91.9 ± 13.9 |

[a] Values given are means ± standard deviations of percentage yields of total activities recovered among the terminal differential sedimentation fractions. Also given are recoveries from the intermediate fractions $S_o$ and $P_1$. Galactosyltransferase was followed in three experiments; other activities were followed in four experiments. Succinate dehydrogenase and arylesterase were measured only in density gradient fractions in these experiments. In preliminary experiments, $P_o$ accounted for 15%, $S_1 + \Sigma S_i$ for 3%, and $\Sigma P_i$ for 83% of the recovered succinate dehydrogenase.

at 250,000 × $g$ × 40 min. For density gradient centrifugation, the intermediate fraction, $P_1$, was resuspended in 25 ml isolation buffer and homogenized in the Tissumiser at low speed for 5 min. Its sorbitol concentration was then brought to 55% by addition of a concentrated sorbitol stock solution [17]. A Beckman Z60 zonal rotor was loaded in the following sequence: an overlay of 20 ml 5% sorbitol; a hyperbolic gradient formed by delivering 180 ml 55% sorbitol through a constant volume mixing chamber initially loaded with 138 ml 30% sorbitol; $P_1$; a hyperbolic gradient formed by delivering 60 ml 65% sorbitol through a mixing chamber initially containing 46 ml 55% sorbitol; and a cushion of 80% sorbitol of sufficient volume to displace 5 ml of the overlay solution. After centrifugation at 240,000 × $g$ × 60 min, the rotor contents were displaced with 80% sucrose and collected in 24 fractions. The density gradient fractions were diluted to 26 ml with isolation buffer and centrifuged at 250,000 × $g$ × 60 min. The resulting pellets, collectively designated $\Sigma P_i$, were resuspended in 2.5 ml isolation buffer; a 1.8 ml aliquot from each fraction was quick-frozen in liquid nitrogen and stored at −70°C until it was subjected to counter-current distribution.

Counter-current distribution was performed at 4°C in the Albertsson thin-layer apparatus [3, 4] as described previously [1, 19]. The phase system contained 5% Dextran T500, 3.5% polyethyleneglycol 6000, 10 μM EDTA, and 8.33 mM imidazole; pH was adjusted with HCl. In most experiments the phase system pH was 6.5. The systems were allowed to equilibrate overnight at 4°C before separation of upper and lower phases.

Marker enzyme and protein determinations were performed on centrifugation and counter-current distribution fractions with the same methods used in previous studies [2, 17].

Marker incremental enrichment factors resulting from individual separation procedures were calculated as the ratios of percentage of recovered marker to percentage of recovered protein. Marker cumulative enrichments were calculated as the products of the incremental enrichment factors obtained in each of the sequence of separation steps [17].

## Results

### Differential and Density Gradient Centrifugation

The homogenization and differential sedimentation procedures were designed to give high yields of the enzymatic markers in the $\Sigma P_i$ sedimentation window. The yield of alkaline phosphatase in $P_o$ was 32%; yields of other enzymatic markers were less than 12%. A wide variability in the $P_o$ alkaline phosphatase yield probably reflects variability in the efficiency with which the cell disruption and subsequent homogenization steps broke intact brush borders into small vesicles. $\Sigma P_i$ contained 50 to 90% yields of the markers listed in Table 1, as well as 83% of the succinate dehydrogenase measured in preliminary experiments.

Figure 2 summarizes marker distributions after a $P_1$ sample was subjected to equilibrium density gradient centrifugation. We routinely divided the density gradients into six windows on the basis of salient features of the marker distribution patterns: Window I contains a portion of the total galactosyltransferase activity relatively well dissociated from the other enzymatic markers. Window II contains membranes with the highest specific activity of Na,K-ATPase. Window III contains plateaus in the distributions of Na,K-ATPase, galactosyltransferase and arylesterase. Windows V and VI together account for most of the recovered alkaline phosphatase and succinate dehydrogenase; these two windows differ markedly, however, in their acid phosphatase and protein contents. Table 2 summarizes the marker contents of the density windows obtained in four experiments.

Alkaline phosphatase had a relatively simple density distribution, consistent with the generally accepted concept that it is concentrated in the brush-border membranes, but small amounts of activity also appear to be associated with membrane populations equilibrating at lower densities. The brush-border membrane population and the mitochondria, marked by succinate dehydrogenase, have almost perfectly overlapping density distributions, but, as summarized in Table 3, they can be separated by a differential rate centrifugation step

**Table 2.** Density distributions of biochemical markers[a]

| | Density window | | | | | |
|---|---|---|---|---|---|---|
| | I | II | III | IV | V | VI |
| Na,K-ATPase | 5.2 ± 1.2 | 42.9 ± 3.2 | 24.9 ± 3.8 | 13.1 ± 2.0 | 10.0 ± 1.6 | 2.9 ± 1.8 |
| Alkaline phosphatase | 1.7 ± 0.8 | 5.2 ± 0.8 | 5.8 ± 1.2 | 9.7 ± 2.9 | 32.85 ± 10.1 | 41.4 ± 12.5 |
| Acid phosphatase | 4.7 ± 1.1 | 21.0 ± 1.0 | 20.9 ± 2.7 | 15.1 ± 4.6 | 21.2 ± 3.2 | 13.6 ± 4.3 |
| Galactosyltransferase | 15.2 ± 5.5 | 28.7 ± 7.4 | 21.8 ± 4.5 | 16.7 ± 4.3 | 11.1 ± 7.0 | 4.6 ± 4.8 |
| Succinate dehydrogenase | 1.6 ± 1.7 | 4.5 ± 3.4 | 4.7 ± 2.1 | 5.0 ± 1.7 | 27.9 ± 19.2 | 38.2 ± 14.7 |
| Arylesterase | 6.3 | 25.6 | 29.2 | 15.8 | 12.6 | 6.8 |
| Protein | 3.8 ± 0.3 | 12.3 ± 1.5 | 13.1 ± 1.1 | 9.7 ± 2.3 | 26.8 ± 10.4 | 22.05 ± 5.3 |

[a] Values given are mean percentage yields ± standard deviations.

**Table 3.** Distribution of markers between microsomal and mitochondrial fractions from Windows V and VI[a]

| | Microsomal fraction | | Mitochondrial fraction | |
|---|---|---|---|---|
| | Window V | Window VI | Window V | Window VI |
| Na,K-ATPase (3) | 80.8 ± 3.5 | 69.4 ± 26.5 | 19.2 ± 3.5 | 30.6 ± 26.5 |
| Alkaline phosphatase (4) | 94.2 ± 3.1 | 93.0 ± 5.7 | 5.8 ± 3.1 | 7.0 ± 5.7 |
| Acid phosphatase (4) | 83.0 ± 7.9 | 77.3 ± 4.7 | 17.0 ± 7.9 | 22.7 ± 4.7 |
| Galactosyltransferase (2) | 63.5 ± 13.6 | 66.4 ± 11.2 | 36.6 ± 13.6 | 33.6 ± 11.2 |
| Succinate dehydrogenase (2) | 23.0 ± 10.7 | 25.4 ± 2.7 | 77.0 ± 10.7 | 74.6 ± 2.7 |
| Arylesterase (1) | 65.1 | 34.9 | 80.0 | 20.0 |
| Protein (4) | 53.6 ± 12.8 | 46.2 ± 6.9 | 46.4 ± 12.8 | 53.8 ± 6.9 |

[a] Values given are mean percentage yields ± standard deviations; number of determinations are given in parentheses. Density Windows V and VI were separated into microsomal and mitochondrial fractions by differential rate centrifugation [18]. One-ml aliquots from each density gradient fraction were pooled, layered over 33-ml columns of 17.5% sorbitol, and centrifuged in an SW-28 rotor at 15,000 rpm for 25 min. The resulting pellet was designated the mitochondrial fraction, and membranes harvested by high-speed centrifugation of the combined sample layer and sorbitol column were designated the microsomal fraction.

with a further 1.8- to 2.0-fold incremental enrichment of alkaline phosphatase. The cumulative enrichment factors for alkaline phosphatase after differential sedimentation, density gradient centrifugation, and differential rate centrifugation were 5.5 from Window V and 9.7 from Window VI. These values are much smaller than the greater than 30-fold enrichment factors observed when brush border membranes were isolated by subfractionation of samples corresponding to $P_o$ [11, 22]. This result suggests that Density Windows V and VI contain one or more additional membrane populations with microsomal sedimentation properties.

Na,K-ATPase, acid phosphatase and arylesterase had multimodal density distributions. This result alone would indicate that each of these markers must be associated with a number of membrane populations which differ on the basis of their density distributions. Na,K-ATPase is primarily associated with a population centered in Density Window II and to a lesser extent with a population centered in Density Window V. The Na,K-ATPase distribution pattern also suggests association with a third population, which is centered in Window III and only partially separated from the major Na,K-ATPase-containing population. The Na,K-ATPase cumulative enrichment factors are 15 in Window II, 8.1 in Window III, and 1.6 in Window V.

The galactosyltransferase density distribution has a major mode between Windows I and II. Although additional density modes are not well-defined, the distribution is heavily skewed toward higher densities, and its shape suggests a summation of contributions by a series of overlapping membrane populations. The cumulative enrichment factor for galactosyltransferase in Window I is 12.

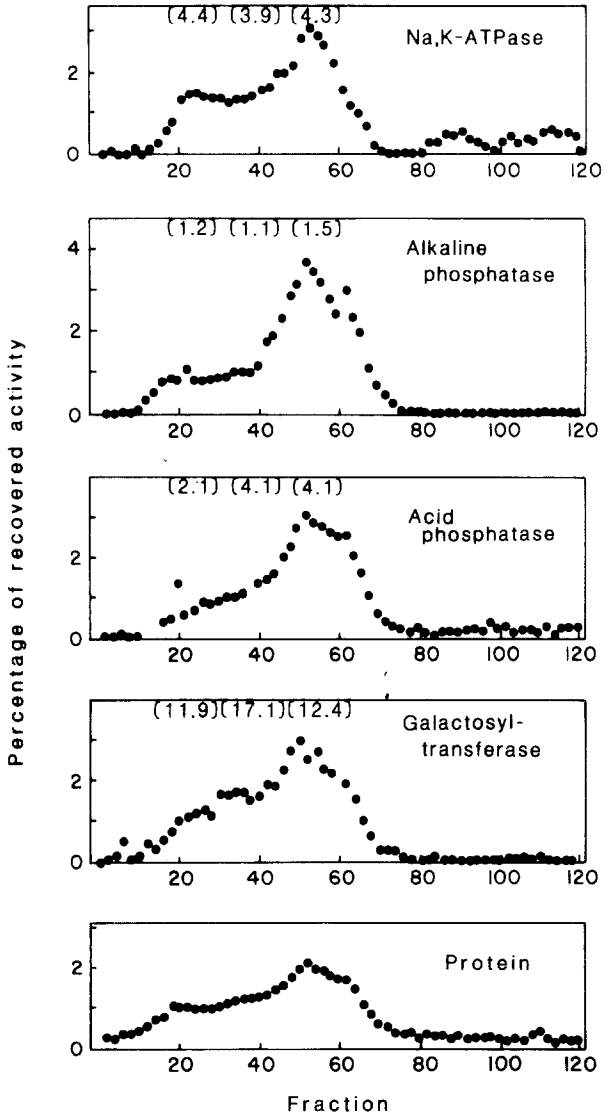


**Fig. 3.** Counter-current distribution analysis of Density Window I. Counter-current distribution was performed as described under Materials and Methods in a two-phase system containing 5% Dextran T500, 3.5% PEG 6000, 5% sorbitol, 10 $\mu$M EDTA, and 8.33 mM imidazole-HCL, pH 6.5. Values in parentheses are marker cumulative enrichment factors calculated for, from left to right, the Very Low-, Low- and Intermediate-Partitioning Windows. Arylesterase was determined in a separate experiment, in which counter-current distribution fractions were pooled into groups of 10 and concentrated 20-fold as described in References [1] and [19]. Given an arbitrary enrichment factor of 1.0 in $\Sigma P_i$, the arylesterase enrichment factors were 2.8, 2.1 and 1.2

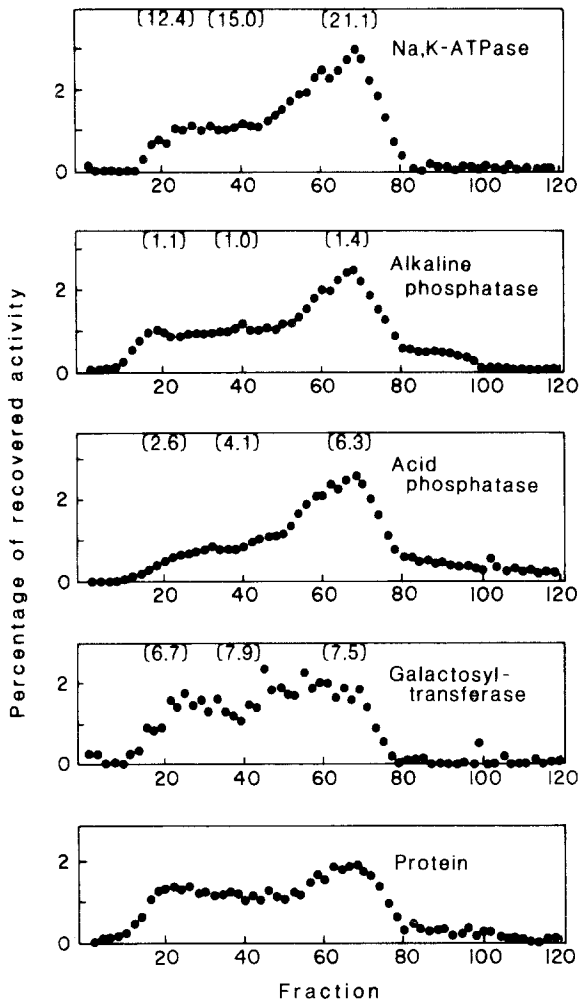


**Fig. 4.** Counter-current distribution analysis of Density Window II. Counter-current distribution was performed as described in the legend to Fig. 3. Values in parentheses are marker cumulative enrichment factors calculated for, from left to right, the Very Low-, Low-, Intermediate- and High-Partitioning Windows. Arylesterase enrichment factors in the Very Low-, Low- and Intermediate Partitioning Windows were 2.8, 2.5 and 2.0

## Counter-Current Distribution

The marker distribution patterns in Fig. 2 lead to two general conclusions: First, most of the enzyme activities we have followed are associated with two or more membrane populations differing on the basis of their modal densities. Second, there is considerable overlap between the density distributions of membrane populations which may differ with respect to marker contents and other physical properties. To learn how the markers are distributed among a possible multiplicity of membrane populations, we analyzed each density window by counter-current distribution in the two-phase system described under Materials and Methods. This analysis, summarized in Figs. 3 through 8, resolved from two to four populations from each density window.

It is necessary to consider both frequency distributions and specific activities of markers in order to delineate a minimum number of membrane populations in the $\Sigma P_i$ sedimentation window. The fre-

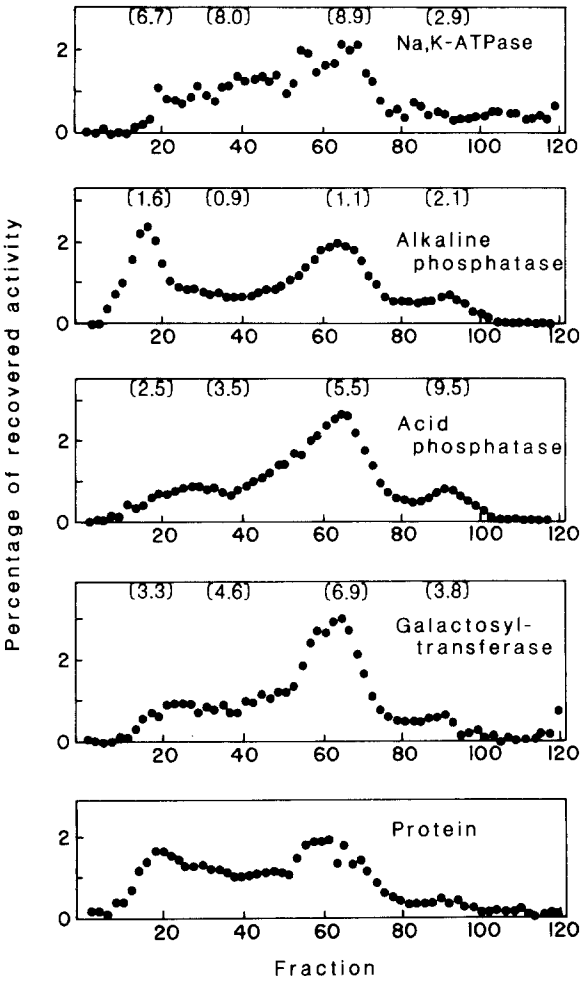


**Fig. 5.** Counter-current distribution analysis of Density Window III. Counter-current distribution was performed as described in the legend to Fig. 3. Arylesterase enrichment factors were 2.7, 2.1, 2.5 and 0.6

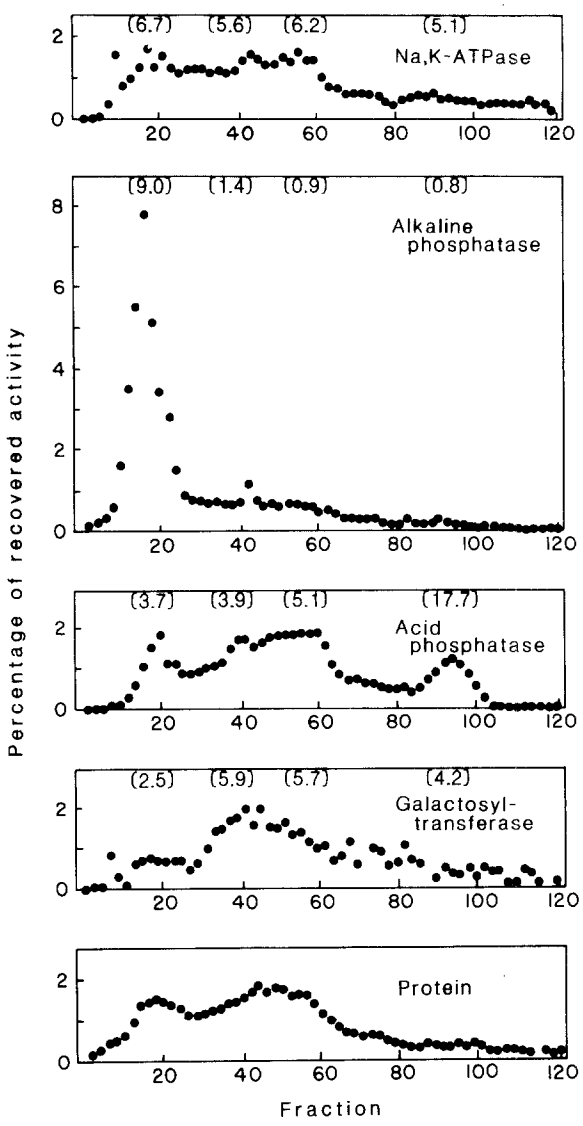


**Fig. 6.** Counter-current distribution analysis of Density Window IV. Counter-current distribution was performed as described in the legend to Fig. 3. Arylesterase enrichment factors were 1.2, 2.4, 1.9 and 0.4

quency distributions from Figs. 1 through 8 are combined in Fig. 9 in the form of a two-dimensional separation. In assembling the specific activities (calculated as cumulative enrichment factors as described under Materials and Methods), we assigned membrane samples to four Partitioning Windows: Very Low Partitioning (fractions 15 to 25); Low Partitioning (fractions 30 to 40); Intermediate Partitioning (fractions 50 to 70); and High Partitioning (fractions 80 to 100). The resulting values are presented with the marker counter-current distribution patterns in Figs. 1 through 8. In using these data to delineate membrane populations, we assigned samples to separate membrane populations if their marker cumulative enrichment factors differed from those of adjacent samples by factors of 2 or greater. Figure 10 summarizes the two-dimensional distributions of membrane populations delineated in this manner.

### *The High Partitioning Window*

The two-dimensional marker distributions in Fig. 9 indicate that acid phosphatase-rich membranes are present from Density Windows III through VI of the High Partitioning Window. The marker cumulative enrichment factors presented in Figs. 5 through 8 indicate that each of these samples is characterized by a unique set of marker cumulative enrichment factors. For example, the cumulative enrichment of acid phosphatase in the High Partitioning sample from Density Window IV is twofold greater than in the other High Partitioning samples. Therefore, the density distributions of markers through the High Partitioning Window reflect a series of four

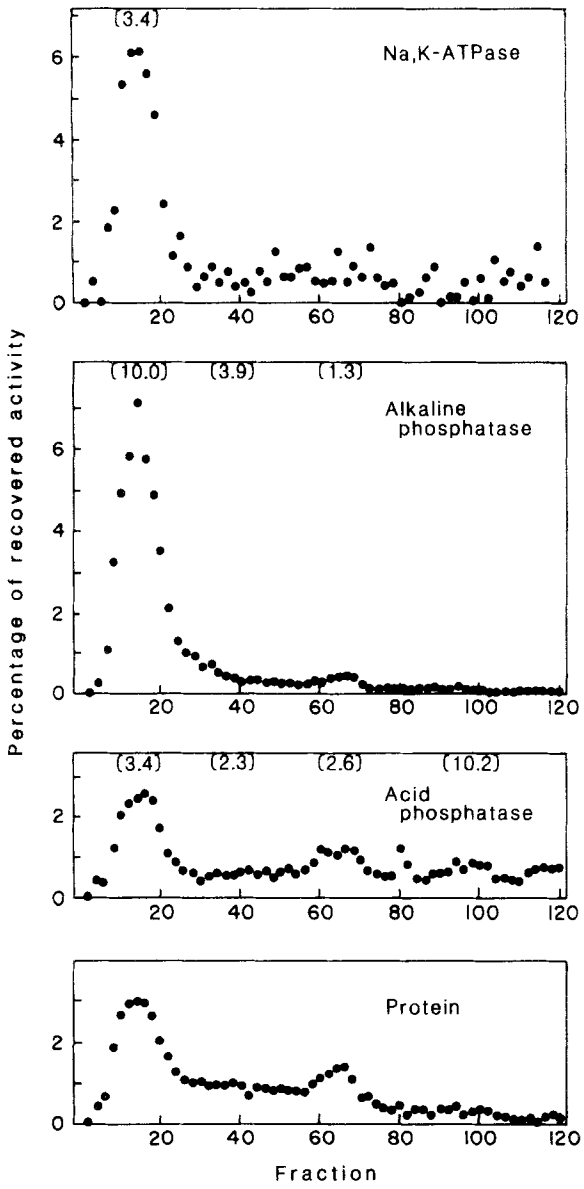


**Fig. 7.** Counter-current distribution analysis of the microsomal elements from Density Window V. Mitochondrial and microsomal fractions were separated as described in the legend to Table 3. Counter-current distribution was performed as described in the legend to Fig. 3. Arylesterase enrichment factors were 0.8, 0.6, 0.2 and 0.4. Galactosyltransferase was also determined in pooled, concentrated fractions from a separate experiment; the resulting enrichment factors were 0.7, 1.3, 0.5 and 1.2

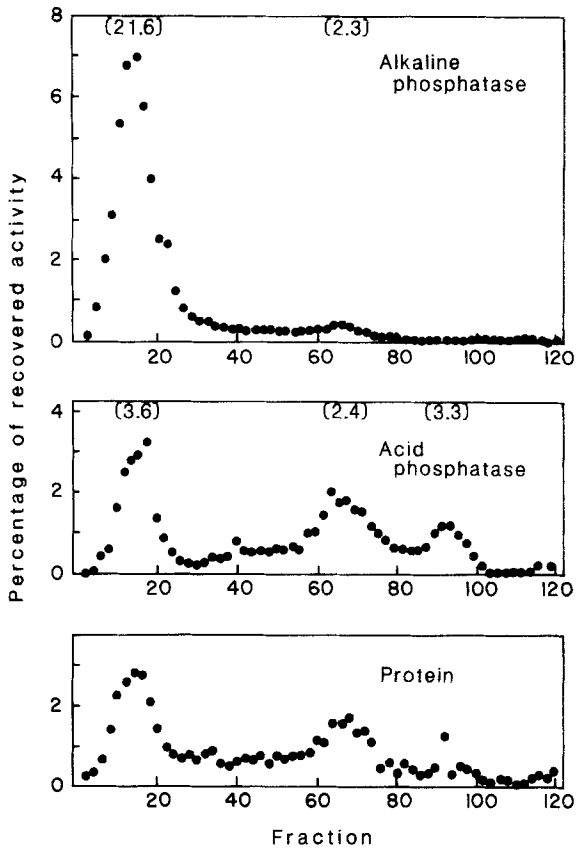


**Fig. 8.** Counter-current distribution analysis of the microsomal elements from Density Window VI. Mitochondrial and microsomal fractions were separated as described in the legend to Table 3. Counter-current distribution was performed as described in the legend to Fig. 3

partially separated membrane populations. These are designated *a*, *b*, *c* and *d* in Fig. 10. Although we have empirically delineated these populations, we cannot yet identify them in terms of their subcellular origins. These populations are conspicuous in Fig. 9 as sites of acid phosphatase activity, and population *b*, with a cumulative enrichment factor of 17, is the locus of the most highly enriched acid phosphatase. These characteristics raise the possibility that the complex of high partitioning membranes has been derived from lysosomes.

### *The Intermediate Partitioning Window*

At least four separate membrane populations are largely contained within the Intermediate Partitioning Window. These are designated *e*, *f*, *g'*, and *h* in Fig. 10. Population *e*, which is centered in Density Window I, can be detected in Fig. 9 as a peak of galactosyltransferase activity. Its galactosyltransferase cumulative enrichment factor of 12.4 raises the possibility that it has been derived from the Golgi complex.

Population *f* is centered in Density Window II. It is apparent as the major peak of Na,K-ATPase activity and it is the locus of the largest Na,K-ATPase cumulative enrichment factor, i.e., 21.1. These characteristics identify population *f* as basal-lateral membrane vesicles.

Population *g'*, centered in Density Window III, appears in Fig. 9 as coinciding peaks in the two-

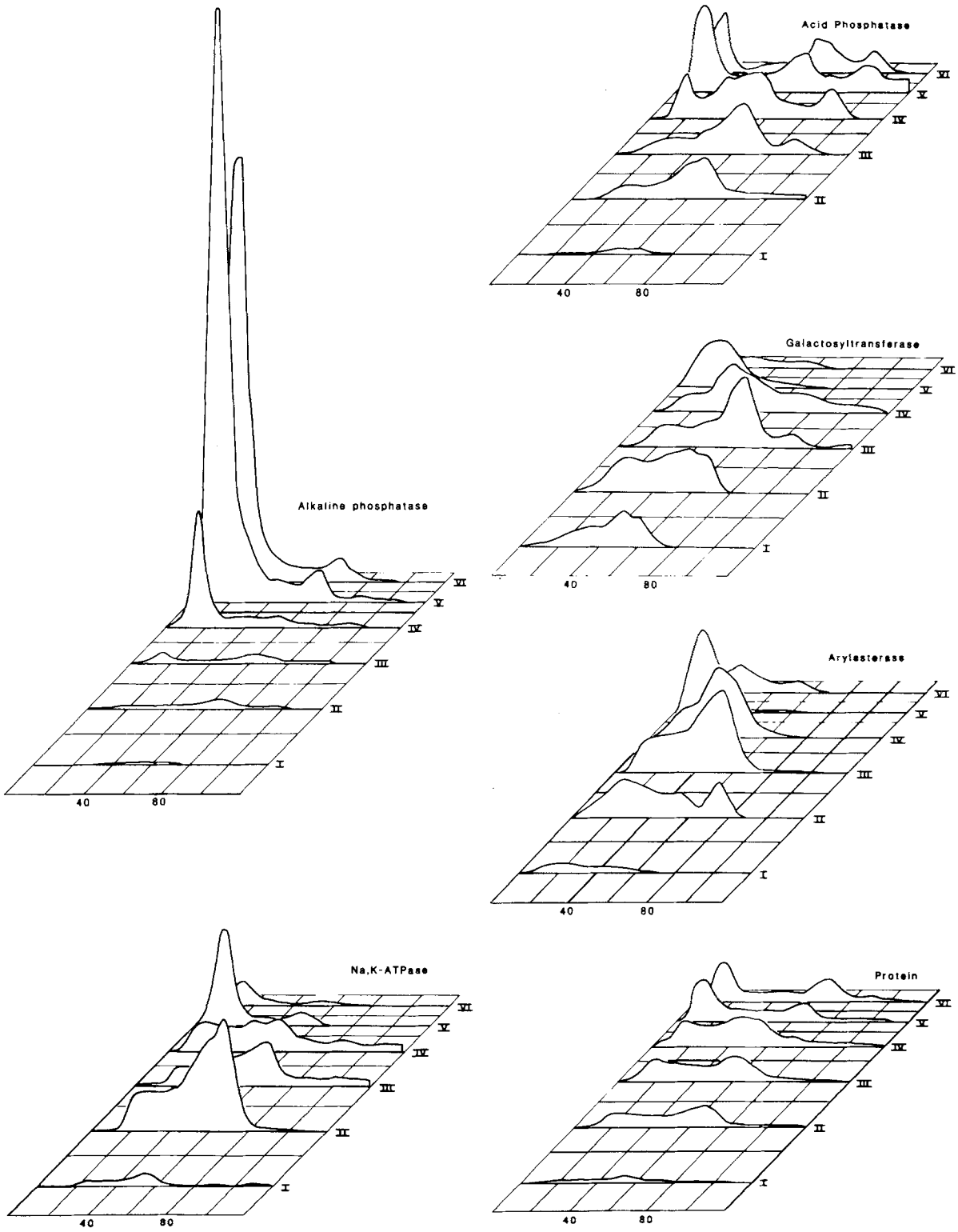


**Fig. 9.** Summary of density gradient and counter-current distribution analyses as a two-dimensional fractionation. Elevations above the Density-Partitioning plane are proportional to percentages of total recovered activity divided by the number of fractions per Density Window. Most data are from Figs. 2 through 8. The following activities are from a separate experiment in which partitioning fractions had been pooled into groups of 10 and concentrated 20-fold as described in References [1] and [19]: arylesterase, all Density Windows; galactosyltransferase, Density Windows V and VI; and Na,K-ATPase, Density Window VI

dimensional distributions of acid phosphatase, arylesterase and, particularly, galactosyltransferase. The fact that population $g'$ has intermediate cumulative enrichment factors for galactosyltransferase (6.9) and arylesterase (2.5) suggests the possibility that it has been derived from less mature elements of the Golgi complex.

Population $h$, spanning Density Windows V and VI, can be visualized from the coinciding peaks in the distributions of alkaline phosphatase and acid phosphatase in Fig. 9. We cannot yet speculate on its possible subcellular origins.

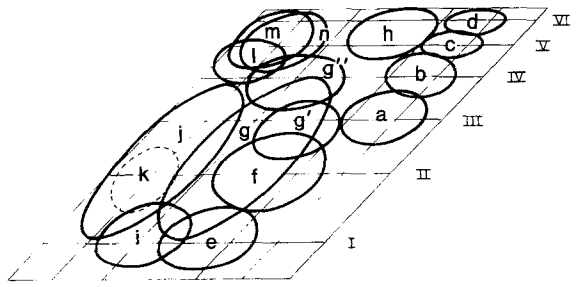


**Fig. 10.** Interpretation of data from Figs. 2–9 in terms of the approximate positions of membrane populations on the Density-Partitioning plane

*The Low Partitioning Window*

Population $i$, centered in Density Window I, appears in Figs. 3 and 9 as a shoulder to the main peak of galactosyltransferase activity in Density Window I. Its marker cumulative enrichment factors distinguish it from population $e$, which represents the major peak of galactosyltransferase in this Density Window. That is, population $i$ has higher cumulative enrichment factors for both galactosyltransferase and arylesterase; with a cumulative enrichment factor of 17.1, population $i$ is the locus of the most highly enriched galactosyltransferase activity, a characteristic which suggests a Golgi origin.

Population $g''$, centered in Density Window IV, can be visualized in Figs. 6 and 9 as peaks in the galactosyltransferase and acid phosphatase distributions. It may be most appropriate to consider populations $g'$ and $g''$ as subpopulations of a single, broadly distributed population centered in the Low Partitioning Window. This population, designated $g$ in Fig. 10, spills into the Intermediate Partitioning Window and spans Density Windows I through IV. Population $g$ is characterized by essentially constant cumulative enrichment factors for alkaline phosphatase, acid phosphatase and arylesterase.

*The Very Low Partitioning Window*

The Very Low Partitioning Window contains a series of five membrane populations. The Very Low Partitioning samples from Density Windows I through III have constant cumulative enrichment factors for alkaline phosphatase, acid phosphatase and arylesterase. These values suggest a single broadly distributed membrane population, which is designated population $j$ in Fig. 10. Population $j$ is the locus of the most highly enriched arylesterase activity, suggesting an endoplasmic reticulum origin. The Very Low Partitioning samples from Density Windows I and II have particularly high enrichment factors for galactosyltransferase. It is possible that this reflects contamination by elements of the galactosyltransferase-rich populations, $g$ and $i$, spilling over from the adjacent, Low Partitioning Window. The Very Low Partitioning sample from Density Window II also has a relatively large cumulative enrichment factor for Na,K-ATPase. We have interpreted this as evidence for the existence of an additional, minor Na,K-ATPase-rich population, which is designated population $k$ in Fig. 10.

The overlap between the striking peak of alkaline phosphatase and the other activities in Density Windows IV through VI of the Very Low Partitioning Window should be interpreted in terms of three distinct but overlapping membrane populations. The cumulative enrichment factors for alkaline phosphatase in the Very Low Partitioning Windows are 9.0 and 10.0 for the samples from Density Windows IV and V, and 21.6 for the sample from Density Window VI.

The alkaline phosphatase cumulative enrichment factors are still somewhat lower than observed in the most highly purified brush-border membrane samples [11, 22]. This result suggests that at least one other population in addition to the brush-border membranes is present in the Very Low Partitioning samples from Density Windows IV through VI. We confirmed this interpretation by performing counter-current distribution at pH 7.6 rather than at pH 6.5; results of such an analysis are summarized in Fig. 11 and in Table 4. The increase in pH preferentially shifted most of the arylesterase and virtually all of the galactosyltransferase activities to the Intermediate and High Partitioning Windows. The populations designated $l$ and $m$ in Fig. 10 represent the membranes which remained in the Very Low Partitioning Window at pH 7.6, and population $n$ represents the arylesterase- and galacto-

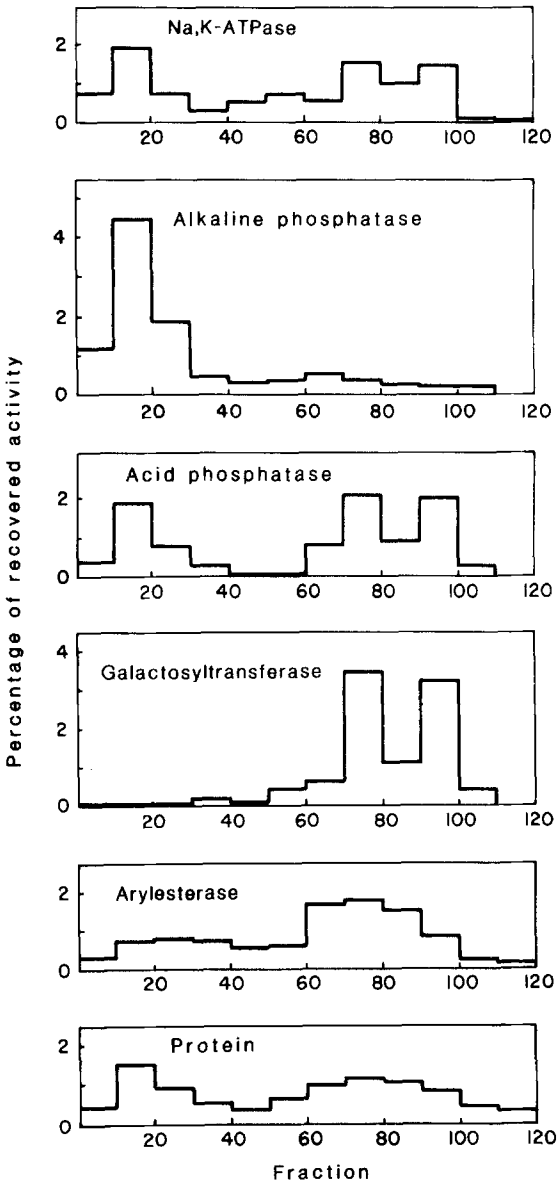


**Fig. 11.** Counter-current distribution analysis of Density Windows V + VI in a two-phase system of pH 7.6; other components of the two-phase system were as described in the legend to Fig. 3. Results are typical of those obtained when each Window was separately analyzed under the same conditions

syltransferase-containing population which moved to the Intermediate and High Partitioning Windows as a result of the pH change. Data in Table 4 emphasize the distinction between populations *l* and *m* since their alkaline phosphatase cumulative enrichment factors differ twofold. The value of 38.4 for population *m*, centered in Window VI, is comparable to previous highly purified brush-border membrane samples. The lower value for population *l*, located in Windows IV and V, suggests the possibility that it might represent a second brush-border membrane population, such as might have been derived from less mature villus cells. However, other explanations are also plausible. For example, population *l* might also represent mixed vesicles which incorporate elements of both the apical and lateral plasma membrane domains.

## Discussion

We have used a total of four different membrane physical properties: sedimentation coefficient, equilibrium density, and aqueous two-phase partitioning at two different pH's, to separate membranes from intestinal mucosal homogenates. On the basis of the resulting distributions of protein and of five different enzyme activities, we have detected 17 different membrane populations. This process has been strictly empirical in the sense that it could be done independently of assumptions about the subcellular localizations of the enzyme activities; the result is a biochemical, as opposed to morphological, atlas of the intestinal epithelial cell.

As we have discussed under Results, the marker contents of several of the isolated populations provide strong clues to their subcellular origins. The mitochondria are contained in the rapidly sedimenting fraction obtained by differential rate sedimentation of Density Windows V and VI. Other populations include: basal-lateral membranes (population *f*), with Na,K-ATPase enriched 21-fold over the initial homogenate; two samples of brush-border membranes (populations *l* and *m*), with alkaline phosphatase cumulative enrichment factors of 14 and 38; two populations derived from the endoplasmic reticulum (*j* and *n*); and a series of populations with characteristics suggesting a Golgi origin (*e*, *i*, *g*, *g'* and *g''*). There are several other membrane samples which we cannot yet identify; these are populations *a*, *b*, *c*, *d*, *h* and *k*. We emphasize, however, that it will be possible to study functional relationships between all the membrane populations we have delineated empirically.

We have recently used the procedures described here to construct a biochemical map of rat exorbital lacrimal gland acinar cells [18, 19]. This map is similar in several respects to Figs. 9 and 10. The position of the exorbital gland basal-lateral membrane population correponds to that of the intestinal basal-lateral membranes (population *f*). The position of the major endoplasmic reticulum population corresponds to population *n*, and the positions of major peaks of galactosyltransferase correspond to populations *g'* and *g''*. The exorbital gland cells also contain a broadly distributed, galactosyltransferase- and NADPH-cytochrome *c* reduc-

tase-rich population corresponding in position to population *g*. Finally, the exorbital gland cells also yield a complex of acid phosphatase-marked populations with positions roughly similar to those of populations *a*, *b*, *c*, *d* and *h*. The most striking difference between the two epithelial cell types is the position of the apical membranes. While intestinal brush-border membranes have relatively high densities and low partition coefficients, the population which most likely represents the exorbital apical membranes has a low density and a high partition coefficient; its position on the density-partitioning plane corresponds to the High Partitioning Window of Density Window II [18, 19].

The map summarized in Figs. 9 and 10 is also congruent with many of the results that have emerged from previous intestinal cell fractionation studies. For example, crude basal-lateral membrane samples corresponding roughly to Density Window II (with Na,K-ATPase enriched 16- to 18-fold) have also been shown to be heterogeneous by third dimension analyses based on cholesterol content, i.e., density perturbation with digitonin [21], and on surface charge, i.e., free-flow [21] and density gradient electrophoresis [24].

The three-dimensional fractionation results provide a framework for interpreting earlier results. One practical conclusion is that density-based partial separation of endoplasmic reticulum- and Golgi-derived samples, such as we have obtained, depends on the density at which the initial sample has been loaded onto the density gradient. An earlier procedure, in which a crude membrane fraction was loaded in the 50% sucrose layer of a discontinuous sucrose gradient, also yielded a partially purified Golgi-derived sample [32]; we would now interpret this sample as a mixture of populations *e* and *i*. In contrast, when fractions corresponding to $P_1$ have been loaded at the low-density ends of density gradients, endoplasmic reticulum- and Golgi-derived populations appear to have largely been compressed into the same density region [2]. Such mixed samples can be resolved by counter-current distribution, and the component populations largely correspond to populations delineated in Figs. 9 and 10 [Ref. 1 and Mircheff and Ahnen, *unpublished*].

The same procedures which yield partially purified, low density Golgi samples also reveal heterogeneity among the populations which contain galactosyltransferase activity. In addition to the partially purified Golgi sample, discontinuous sucrose gradients also contained a second, higher density peak of galactosyltransferase [32]. This peak overlapped the major peak of Na,K-ATPase, and the relationship between these two markers implied that basal-lateral, as well as Golgi, membranes contained galactosyltransferase [32]. The two-dimensional marker distributions in Fig. 9 partially support this conclusion, but they also lead to more complex interpretations of the subcellular organization of both Na,K-ATPase and galactosyltransferase. A parallel between the Na,K-ATPase and galactosyltransferase distributions between fractions 60 and 70 in Fig. 4 tends to confirm the conclusion that some galactosyltransferase is associated with the basal-lateral membranes. Parallels between Na,K-ATPase and galactosyltransferase in other regions of the Density-Partitioning plane indicate that Na,K-ATPase also has a complex subcellular distribution, being associated with Golgi-derived populations *g*, *g'* and *g''* and with endoplasmic reticulum-derived populations *j* and *n*. While this complexity has not been suspected previously, it would account for the frequent observation that Na,K-ATPase distributions are skewed toward higher densities [2, 22]; it would also explain the overlap between bimodal distributions of Na,K-ATPase and NADPH-cytochrome *c* reductase after a crude basal-lateral membrane fraction had been analyzed by free-flow electrophoresis [21].

Despite the general consistency between the pictures of intracellular biochemical organization emerging from different fractionation methods, it is necessary to re-examine some of the conclusions drawn from studies which have relied entirely on centrifugation procedures. In pulse-labeling experi-

**Table 4.** Cumulative enrichment factors after counter-current distribution at pH 7.6[a]

| | Partitioning window | | |
|---|---|---|---|
| | Very Low | Intermediate | High |
| Na,K-ATPase | | | |
| Density Window V | 3.5 | 0.7 | 3.5 |
| Density Window VI | 2.1 | 0.6 | 0.8 |
| Alkaline Phosphatase | | | |
| Density Window V | 14.3 | 2.4 | 7.8 |
| Density Window VI | 38.4 | 3.0 | 0.9 |
| Acid Phosphatase | | | |
| Density Window V | 1.8 | 1.8 | 7.7 |
| Density Window VI | 3.5 | 3.6 | 5.4 |
| Galactosyltransferase | | | |
| Density Window V | 0.7 | 0.9 | 3.7 |
| Density Window VI | 0.1 | — | — |
| Arylesterase | | | |
| Density Window V | 0.3 | 0.8 | 0.5 |
| Density Window VI | 0.1 | 0.3 | 0.2 |

[a] Cumulative enrichment factors after microsomal elements from Density Windows V and VI had been subjected to counter-current distribution at pH 7.6. Other details are described in the text and legend to Table 3.

ments border-destined glycoproteins appeared in basal-lateral membrane-containing density gradient fractions before being incorporated into the brush-border membranes [26, 27]. This result implied that the basal-lateral membranes mediate a significant component of the flux of newly synthesized glycoproteins between the Golgi complex and the brush border. It now appears that the quantitative significance of this transit route may be much smaller than originally envisioned, since substantial fractions of the newly incorporated label may well have been associated with elements of the Golgi-derived populations $g$ and $g'$ rather than with the basal-lateral membranes.

The observation that populations of endoplasmic reticulum- and Golgi-derived membranes have density distributions similar to the basal-lateral membranes also suggests that it may be appropriate to re-examine the results of experiments in which isolated basal-lateral membrane samples have been used to probe transepithelial transport mechanisms. One topic of interest is ATP-driven calcium transport. This process has been detected and thoroughly characterized in basal-lateral membrane samples [12, 13, 14, 23]. Its kinetic properties and sensitivity to vitamin D status are consistent with the conclusion that it represents a basal-lateral membrane-localized calcium pump. On the other hand, studies of neural and hormonal regulation of NaCl absorption [8, 9] lead to the conclusion that intestinal cells, like secretory epithelial cells [e.g., 30, 33] possess intracellular compartments which actively accumulate calcium. Since both endoplasmic reticulum and Golgi membranes may participate in calcium sequestration in exocrine acinar cells [20], it will be interesting to learn whether the ATP-dependent calcium transport activity measured in isolated basal-lateral membrane samples might actually be shared between the basal-lateral membrane population and previously unsuspected Golgi- and endoplasmic reticulum-derived populations.

The results of this study also point to several possible new directions. For example, Fig. 10 provides a map with which one might attempt to trace the intracellular transit of plasma membrane-destined proteins. Na,K-ATPase is especially prominent among these, since the size of its intracellular pool is so large in comparison to the intracellular alkaline phosphatase pool. To some extent this activity may reflect newly synthesized enzyme en route to the basal-lateral membrane. It is conceivable, however, that some portion of this activity might represent a reserve capacity, available for recruitment to the plasma membranes in a mechanism analogous to that of insulin-mediated stimulation of plasma membrane glucose transport activity [e.g., 6]. Such a process could be imagined to participate in the cell's ability to buffer cytosolic sodium activity when the presence of luminal sugars and amino acids accelerate sodium influx across the brush-border membrane [*cf.* 29].

This work was supported by NIH Grants AM28408 and AM11270, and by NSF Grant PCM 7911030.

## References

1. Ahnen, D.J., Mircheff, A.K., Santiago, N.A., Yoshioka, C., Gray, G.M. 1983. Intestinal surface aminooligopeptidase. Distinct molecular forms during assembly on intracellular membranes *in vivo*. *J. Biol. Chem.* **258:**5960–5966
2. Ahnen, D.J., Santiago, N.A., Cezard, J.-P., Gray, G.M. 1982. Intestinal aminooligopeptidase. *In vivo* synthesis on intracellular membranes of rat jejunum. *J. Biol. Chem.* **257:**12129–12135
3. Albertsson, P.Å. 1970. Separation of cells and cell particles by counter-current distribution. *Sci. Tools* **17:**53–57
4. Albertsson, P.Å., Andersson, B., Larsson, C., Akerlund, H.-E. 1982. Phase partition. A method for purification and analysis of cell organelles and membrane vesicles. *Methods Biochem. Anal.* **28:**115–150
5. Cezard, J.-P., Conklin, K.A., Das, B.C., Gray, G.M. 1979. Incomplete intracellular forms of intestinal surface membrane sucrase-isomaltase. *J. Biol. Chem.* **254:**8969–8975.
6. Cushman, S.W., Wardazla, L.J. 1980. Potential mechanism of insulin action on glucose transport in the isolated rat adipose cell: Apparent translocation of intracellular transport systems to the plasma membrane. *J. Biol. Chem.* **255:**4758–4762
7. DeDuve, C. 1964. Principles of tissue fractionation. *J. Theor. Biol.* **6:**33–59
8. Donowitz, M. 1983. $Ca^{2+}$ in the control of active intestinal Na and Cl transport: Involvement in neurohumoral action. *Am. J. Physiol.* **245:**G165–G177
9. Donowitz, M., Cusolito, S., Battisti, L., Sharp, G.W.G. 1983. Dantrolene and basal ileal sodium and chloride transport: Involvement of calcium stores. *Am. J. Physiol.* **245:**G780–G785
10. Farquhar, M.G., Palade, G.E. 1981. The Golgi apparatus (complex)-(1954–1981)-from artifact to center stage. *J. Cell Biol.* **91:**773–1035
11. Forstner, G.G., Sabesin, S.M., Isselbacher, K.J. 1968. Rat intestinal microvillus membranes. Purification and biochemical characterization. *Biochem. J.* **106:**381–390
12. Ghijsen, W.E.J.M., Jong, M.D. de, Os, C.H. van 1982. ATP-dependent calcium transport and its correlation with $Ca^{2+}$-ATPase activity in basolateral plasma membranes of rat duodenum. *Biochim. Biophys. Acta* **689:**327–336
13. Ghijsen, W.E.J.M., Os, C.H. van 1982. 1$\alpha$,25-dihydroxyvitamin D3 regulates ATP-dependent calcium transport in basolateral plasma membranes of rat enterocytes. *Biochim. Biophys. Acta* **689:**170–172
14. Hildmann, B., Schmidt, A., Murer, H. 1982. $Ca^{++}$ transport across basal-lateral plasma membranes from rat small intestinal epithelial cells. *J. Membrane Biol.* **65:**55–62

15. Miller, D., Crane, R.K. 1961. The digestive function of the epithelium of small intestine. II. Localization of disaccharide hydrolases in the isolated brush border portion of intestinal epithelial cells. *Biochim. Biophys. Acta* **52:**293–298
16. Mircheff, A.K. 1983. Empirical strategy for analytical fractionation of intestinal epithelial cells. *Am. J. Physiol.* **244:**G347–G356
17. Mircheff, A.K., Conteas, C.N., Lu, C.C., Santiago, N.A., Gray, G.M., Lipson, L.G. 1983. Basal-lateral and intracellular membrane populations of rat exorbital lacrimal gland. *Am. J. Physiol.* **245:**G133–G142
18. Mircheff, A.K., Lu, C.C. 1984. A map of membrane populations isolated from rat exorbital gland. *Am. J. Physiol.* (*In press*)
19. Mircheff, A.K., Lu, C.C., Conteas, C.N. 1983. Resolution of apical and basal-lateral membrane populations from rat exorbital gland. *Am. J. Physiol.* **245:**G661–G667
20. Mircheff, A.K., Os, C.H. van, Lu, C.C. 1984. Subcellular distribution of ATP-dependent calcium transport in exorbital gland. *In:* Proceedings of the First International Tear Film Symposium. F.J. Holly, editor. (*in press*)
21. Mircheff, A.K., Sachs, G., Hanna, S.D., Labiner, C.S., Rabon, E., Douglas, A.P., Walling, M.W., Wright, E.M. 1979. Highly purified basal lateral plasma membranes from rat duodenum. Physical criteria for purity. *J. Membrane Biol.* **50:**343–363
22. Mircheff, A.K., Wright, E.M. 1976. Analytical isolation of plasma membranes of intestinal epithelial cells. Identification of Na,K-ATPase rich membranes and the distribution of enzyme activities. *J. Membrane Biol.* **28:**309–333
23. Nellans, H., Popovitch, J.E. 1981. Calmodulin-regulated, ATP-driven calcium transport by basolateral membranes of rat small intestine. *J. Biol. Chem.* **256:**9932–9936
24. Os, C.H. van, Jonge, H.R. de, Jong, M.D. de, Ghijsen, W.E.J.M., Walters, J.A.L.I. 1980. Separation of basolateral plasma membranes from smooth endoplasmic reticulum of the rat enterocyte by zonal electrophoresis on density gradients. *Biochim. Biophys. Acta* **600:**730–738
25. Pastan, I.H., Willingham, M.C. 1981. Journey to the center of the cell: Role of the receptosome. *Science* **214:**504–509
26. Quaroni, A., Kirsch, K., Weiser, M.M. 1979. Synthesis of membrane glycoproteins in rat small-intestinal villus cells. Redistribution of L-($^3$H)-fucose-labelled membrane glycoproteins among Golgi, lateral basal, and microvillus membranes *in vivo*. *Biochem. J.* **182:**203–212
27. Quaroni, A., Kirsch, K., Weiser, M.M. 1979. Synthesis of membrane glycoproteins in rat small-intestinal villus cells. Effect of colchicine on the redistribution of L-($^3$H)-fucose-labelled membrane glycoproteins among Golgi, lateral basal, and microvillus membranes. *Biochem. J.* **182:**213–221
28. Schultz, S.G. 1979. Sodium-coupled solute transport by small intestine: A status report. *Am. J. Physiol.* **233:**E249–E254
29. Schultz, S.G. 1981. Homocellular regulatory mechanisms in sodium-transporting epithelia: Avoidance of extinction by "flush-through." *Am. J. Physiol.* **241:**F579–F590
30. Schulz, I. 1980. Messenger role of calcium in function of pancreatic acinar cells. *Am. J. Physiol.* **239:**G335–G347
31. Weiser, M.M. 1973. Intestinal epithelial cell surface membrane glycoprotein synthesis. I. An indicator of cellular differentiation. *J. Biol. Chem.* **248:**2536–2541
32. Weiser, M.M., Neumeier, M.M., Quaroni, A., Kirsch, K. 1978. Synthesis of plasmalemmal glycoproteins in intestinal epithelial cells. Separation of Golgi membranes from villus and crypt cell surface membranes; galactosyltransferase activity of surface membrane. *J. Cell Biol.* **77:**722–734
33. Williams, J.A. 1980. Regulation of pancreatic acinar cell function by intracellular calcium. *Am. J. Physiol.* **238:**G269–G279

Received 13 April 1984; revised 16 July 1984